INTERNATIONAL SOCIETY FOR
SOIL MECHANICS AND
GEOTECHNICAL ENGINEERING

SIMSG ISSMGE

This paper was downloaded from the Online Library of the International Society for Soil Mechanics and Geotechnical Engineering (ISSMGE). The library is available here:

https://www.issmge.org/publications/online-library

This is an open-access database that archives thousands of papers published under the Auspices of the ISSMGE.

The paper was published in the proceedings of the 11th International Conference on Physical Modelling in Geotechnics (ICPMG2026) and was edited by Ioannis Anastasopoulos. The conference was held from June 8th to June 12th 2026 in Zurich, Switzerland.

Proceedings of the 11th ICPMG 2026
11th International Conference on Physical Modelling in Geotechnics
8-12 June 2026, Zurich, Switzerland
© 2026 the Authors

Numerical Analysis of Geotechnical Seismic Isolation Using Expanded Polystyrene: Application to the EuroProteas Prototype at the Euroseistest Site

M.P.A. Gatto
University of Brescia, Brescia, Italy, michele.gatto@unibs.it

L. Montrasio
University of Brescia, Brescia, Italy, lorella.montrasio@unibs.it

C. Amendola, E. Filoglou, D. Pitilakis
Aristotle University of Thessaloniki, Thessaloniki, Greece, chiaamen@civil.auth.gr, elenfilo@civil.auth.gr, dpitilakis@civil.auth.gr

H.H. Tsang
University of Dundee, Dundee, United Kingdom, HTsang001@dundee.ac.uk

ABSTRACT: This paper presents numerical analyses developed to support full-scale physical modelling of an expanded polystyrene (EPS) layer used as a geotechnical seismic isolation (GSI) system beneath a prototype structure at the EuroSeisTest site. The study focuses on the EuroProteas structure, a well-instrumented full-scale facility designed to investigate dynamic soil–foundation–structure interaction through free and forced vibration tests. A two-dimensional finite element model was developed in PLAXIS and calibrated against existing experimental data obtained without EPS, with particular attention to the soil–structure interface behaviour under dynamic loading. The calibrated model was then employed to predict the static and dynamic response of the system after introducing a 0.5 m thick EPS layer beneath the foundation. Numerical results indicate that the EPS layer does not experience excessive deformation under static loading and induces a significant modification of the coupled system's dynamic response, including a reduction of resonant frequencies and structural accelerations. Two alternative sets of EPS deformability parameters, derived from laboratory testing, were considered to bracket the expected response. The analyses provide quantitative insight into the mechanisms governing wave propagation and energy transfer in EPS-based GSI systems and serve as a predictive framework for the design, interpretation, and validation of upcoming full-scale experimental tests. The results highlight the role of numerical modelling as an essential complement to physical modelling in advancing innovative seismic isolation solutions.

1 INTRODUCTION

Seismic risk mitigation remains a key challenge in geotechnical and structural engineering, particularly for existing structures where interventions on the superstructure may be costly, invasive, or impractical. In this context, Geotechnical Seismic Isolation (GSI) has emerged as a promising alternative strategy, aiming to reduce seismic demand at the foundation level through engineered soil modifications or the inclusion of isolation layers. Unlike conventional isolation techniques applied directly to the structure, GSI enables risk reduction without altering the superstructure, offering a cost-effective and potentially more resilient solution for both new and existing buildings. A recent comprehensive review by Tsang (2025) has highlighted the potential of GSI, while also emphasizing the technical challenges that must be addressed for its widespread implementation.

Among the various GSI techniques, the use of lightweight polymer-based materials, such as Expanded Polystyrene (EPS) and polyurethane foams, has gained increasing attention. These materials exhibit favourable mechanical properties, low density, and ease of installation, making them attractive candidates for practical application in seismic isolation. Previous studies conducted by University of Brescia have investigated the seismic isolation potential of polyurethane layers at the laboratory scale, demonstrating their ability to attenuate seismic waves and modify the dynamic response of soil–structure systems (Montrasio and Gatto 2016; Gatto et al. 2021; Gatto et al. 2022; Gatto and Montrasio 2023). Despite these promising findings, full-scale experimental validation is still lacking, and the real-world effectiveness of polymer-based GSI solutions remains an open question.

To address this gap, full-scale experimental tests are planned within the framework of the ERIES project, leveraging the EuroProteas prototype structure at the EuroSeisTest site in Greece—a well-instrumented facility dedicated to Soil–Foundation–Structure Interaction (SFSI) studies (Pitilakis et al. 2013; Pitilakis et al. 2018). This structure has recently been used for testing GSI solutions incorporating rubber layers (Pitilakis et al. 2021; Pitilakis et al. 2024). In the planned campaign, free and forced vibration tests will be conducted with an EPS slab installed beneath the foundation slab, aiming to evaluate its influence on the dynamic response of the soil–structure system under seismic loading.

In preparation for the large-scale experimental tests, this study presents preliminary numerical simulations using a finite element model developed in PLAXIS 2D, calibrated against previous experimental data obtained without the EPS layer. The simulations serve multiple purposes: they support the design of the upcoming tests, help refine key modelling assumptions, and provide a reference for interpreting future experimental results. By anticipating the experimental campaign, this work offers preliminary insight into the potential effectiveness of polymer-based GSI systems at full scale and contributes to the development of robust modelling strategies for their future validation and application in seismic risk mitigation.

2 EXPERIMENTAL SETUP AND FINITE ELEMENT MODELLING OF THE DYNAMIC SFSI IN EUROPROTEAS STRUCTURE

2.1 Description of the Experimental Setup

The EuroProteas structure consists of four QHS 160×10 steel columns, each 3.8 meters tall, which are rigidly connected to reinforced concrete slabs at both the top and the bottom. Each slab measures 3×3 meters and has a thickness of 40 cm; the bottom slab serves as the foundation, while the top consists of one or two roof slabs, resulting in a total thickness of 40 cm or 80 cm depending on the configuration. Two optional X-braces (2L80×60) can be installed to alter the structural stiffness. The overall layout of the structure is shown in Figure 1a.

The geotechnical profile of the soil beneath the structure was investigated through two boreholes: BH1, located 0.5 meters from the structure's edge, and BH2, positioned at its center. BH1 was drilled to a depth of 15 meters, while BH2 reached 30 meters. Standard Penetration Tests (SPT) were conducted in both boreholes, whereas down-hole tests were performed only in BH2. Soil samples extracted from the boreholes underwent classification tests as well as direct shear and resonant column tests. These laboratory investigations provided essential mechanical parameters, including grain-size distribution, strength parameters for fine-grained soils, and modulus reduction and damping curves. Further details on the geotechnical investigation can be found in Pitilakis et al. (1999).

EuroProteas was specifically designed to investigate SFSI under dynamic loading conditions, offering a controlled environment for full-scale experimental studies. Within this facility, both free vibration and forced vibration tests can be conducted. In free vibration tests, the structure is connected to the ground via a rope, which is pulled to displace the structure and then suddenly released by cutting the rope, allowing the structure to oscillate freely (Figure 1b). This setup enables observation of the natural dynamic response of the soil–structure system without continuous external forcing. In forced vibration tests, a horizontal sinusoidal load is applied to the top of the structure using rotating masses (Figure 1c). The excitation frequency can be precisely controlled from 1 to 10 Hz, and the magnitude of the applied load can be adjusted by placing additional plates on top of the rotating masses, allowing for 1 to 4 plates to be used to vary the force amplitude.

Figure 1. Overview of the EuroProteas experimental setup: (a) general view of the structure, (b) detail of the devices attached at the top of the structure for free vibration testing, and (c) rotating masses used to induce forced vibration.

2.2 Numerical modelling

The numerical simulations were conducted using a two-dimensional finite element model developed in

PLAXIS 2D. The structural components of EuroProteas, including the steel columns, X-braces, and concrete slabs, were modelled using elastic plate elements. These elements require the definition of axial and flexural stiffness—namely, EA and EI—as well as the unit weight of the material. The unit weight was computed as the product of the material's volumetric weight (25 kN/m3 for concrete, 75 kN/m3 for steel) and the out-of-plane dimension, which was set to 0.1 meters for steel elements and 3 meters for concrete slabs, in accordance with the 2D modelling assumptions. Although the unit weight of steel has a limited influence on the stress state in the foundation, assigning it a value of zero would lead to an inaccurate representation of structural deformation and energy dissipation. Material damping was introduced using the Rayleigh damping approach, based on typical damping ratios for steel and concrete structures, and consistent with the frequency range observed in the experimental tests. The cross-sectional properties (area, moments of inertia), and calculated stiffnesses for all structural elements are summarized in Table 1.

Table 1. Geometrical properties and stiffness parameters of the structural elements of EuroProteas.

Structural element	Cross section area *A* (m²)	Moment of inertia *I* (m⁴)	Axial rigidity *EA* (kN)	Flexural Rigidity *EI* (kNm²)
Column	$5.3\cdot10^{-3}$	$1.65\cdot10^{-5}$	$1.1\cdot10^{6}$	3471
X-braces	$1.9\cdot10^{-3}$	$0.17\cdot10^{-5}$	4.03	371.7
Foundation	0.4	0.005	$1.2\cdot10^{7}$	$0.16\cdot10^{6}$
Roof	0.8	0.043	$2.4\cdot10^{7}$	$1.28\cdot10^{6}$

The soil domain was discretized to a depth of 30 meters and a width of 120 meters to minimize boundary effects on the dynamic response of the soil-structure system. Absorbing boundary conditions were applied via rollers with horizontal axes on the lateral sides and rollers with vertical axes at the base, acting as viscous dampers to reduce spurious wave reflections, following the approach of Lysmer and Kuhlemeyer (1969) as implemented in PLAXIS.

Soil behaviour was simulated using the Hardening Soil model with Small-Strain stiffness (HS small), which features non-linear stiffness degradation. This allows for a realistic representation of soil response under dynamic loading at small to intermediate strain levels. The model is elasto-plastic and employs the Mohr–Coulomb failure criterion. In PLAXIS, the HS small model automatically derives strain-dependent hysteretic damping from the modulus reduction curve (G/G_0). However, Rayleigh damping parameters are also required to account for viscous damping effects at very low strains and higher vibration modes. Together, these provide a complete representation of soil damping under dynamic loading.

Based on borehole and laboratory data, five stratigraphic layers were identified: the upper two consisting of fine-grained cohesive soils (mainly clayey), and the lower three composed of coarse-grained materials (mainly sands and gravels). With the groundwater table at 1.7 m depth and considering typical foundation influence depths from Boussinesq elastic solutions for a 3 m × 3 m foundation, undrained conditions (Type B) were assumed for the upper cohesive layers, and drained conditions for the underlying coarse-grained strata. Undrained shear strength su for clayey soils in undrained conditions were derived from unconsolidated undrained triaxial (TXUU) tests (su = 65 kPa), while strength parameters for coarse soils were estimated from SPT and laboratory direct shear tests, resulting in friction angles $\phi' = 36.5°$ for layer 3 and $\phi' = 38.6°$ for layers 4 and 5.

For deformability, the HS small model requires the small-strain shear modulus G0, secant stiffness E50, oedometer stiffness Eoed, and unloading-reloading stiffness Eur, all referenced to a confining pressure. G0 was derived from the down-hole shear wave velocity profile using $G0=\rho\cdot v_s^2$, assuming a Poisson's ratio $\nu = 0.25$ for all layers. Young's modulus E0 was then derived from G0 based on elastic theory and E50 was back-calculated using the stiffness ratio E0/E50 = 8.55, recommended by Obrzud and Truty (2018) for fine-grained soils. Eoed followed from standard elastic relations, and E_{ur} was set equal to 4·E50. The modulus reduction curve was defined using a hyperbolic model, with $\gamma 0.7$ fitted to resonant column test results. Table 2 reports geometrical and stiffness properties for each layer. All stiffness parameters are referenced to a confining pressure equal to the representative mean isotropic stress within each layer.

Table 2. Geotechnical and stiffness properties of soil layers: depth (z), shear wave velocity (v_s), small-strain shear modulus (G_0), secant stiffness (E_{50}), oedometer stiffness (E_{oed}), and reference shear strain ($\gamma_{0.7}$).

Layer	*z* (m)	v_s (m/s)	G_0 (kPa)	E_{50} (kPa)	E_{oed} (kPa)	$\gamma_{0.7}$ (%)
1	0-0.5	100	20489	5991	7189	0.018
2	0.5-3	150	46101	13480	16176	0.018
3	3-8	175	64934	18986	22784	0.021
4	8-17	155	51626	15095	18114	0.018
5	17-30	180	66551	19459	23351	0.018

The soil domain was discretized using 15-node triangular elements under plane strain conditions. Mesh refinement was guided by the Kuhlmeyer and Lysmer criterion to prevent numerical dispersion. Specifically, the maximum allowable element size Δx was calculated as Δx ≤ vs,min / (10 fmax). With a minimum shear wave velocity vs,min of 100 m/s and a maximum frequency fmax of 10 Hz, the maximum element size was set to 1 meter. An excerpt of the numerical model, including the plate elements for the structure, the triangular soil elements, and the interface elements, is shown in Figure 2. For time integration in the dynamic analyses, the Courant-Friedrichs-Lewy (CFL) condition was satisfied by choosing a time step Δt = 0.006 s, ensuring numerical stability given the highest shear wave velocity and minimum element size in the domain.

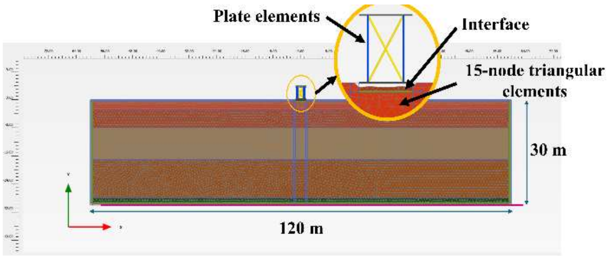

Figure 2. Numerical model excerpt showing the plate elements representing the structure, triangular elements discretizing the soil domain, and the interface elements between soil and structure.

A key aspect of the modelling was the soil-structure interface, which significantly influences the dynamic response of the coupled system. In PLAXIS, the interface behaviour is governed by two parameters: the virtual thickness (*VT*) and the interface strength reduction factor (R_{inter}). *VT* represents a notional thickness assigned to the interface element, affecting its deformability, while R_{inter} modifies the strength and stiffness properties of the interface relative to the adjacent soil. Both parameters were calibrated specifically for the concrete-soil contact through a parametric analysis.

Although the analyses were conducted in 2D plane strain, the calibration was verified against the key global response indicators from the 3D full-scale tests, ensuring that the selected parameters remained representative of the actual system behaviour.

2.3 Calibration of the interface parameters based on previous experimental tests on EuroProteas without EPS

To calibrate the numerical model, with particular focus on the interface parameters, we simulated both free vibration and forced vibration tests from a previous experimental campaign conducted without EPS material, as documented in Pitilakis et al. (2013). As described in Section 2.1, the free vibration tests consisted of displacing the structure by tensioning and suddenly releasing a rope attached near its top. Prior to release, three distinct point loads F were applied: 1.18 kN, 2.65 kN, and 4.77 kN. In the numerical model, free vibration was simulated by applying a point load at one end of the roof slab, matching the experimental force magnitude, and then releasing it. In PLAXIS, this was modeled as a line load (force per unit length) applied out-of-plane (in the z-direction) on the plate element. Because the physical load was applied at the mid-depth of the slab, the total forces were divided by the slab thickness (1.5 m) to obtain equivalent line loads.

For calibration, we focused on the lowest load case (F=1.18 kN), adopting a strength reduction factor Rinter=0.8, which is appropriate for concrete-to-soil contacts (Teshome 2025). The virtual thickness VT was varied among four values: 0.05, 0.07, 0.08, and 0.1. Figure 3 compares numerical and experimental results for horizontal accelerations and their corresponding Fast Fourier Transforms (FFT). The fundamental frequency from the numerical model (3.1–3.2 Hz) closely matches the experimental value for all VT values, while the best amplitude fit is achieved at VT=0.07. The secondary peak around 10 Hz corresponds to a higher-order mode related to local bending of the slab and soil–structure interaction. Using the calibrated parameters Rinter=0.8 and VT=0.07, Figure 4 presents numerical–experimental comparisons for all three load magnitudes, both in terms of accelerations and FFT. Good agreement is observed overall. However, for the highest load (F=4.77 kN), a slight decrease in the experimental fundamental frequency is noted, which is not captured by the numerical model, where the frequency response remains load-invariant.

Following the free vibration analysis, forced vibration tests were simulated for two cases with three steel plates in the rotating masses, at rotation frequencies of 3 Hz and 5 Hz, corresponding to force amplitudes F = 2.46 kN and F = 6.84 kN, respectively. As before, total forces were divided by the slab thickness (1.5 m) to obtain the line load applied to the plate element. Unlike the free vibration case, the load was applied horizontally at the centre node of the roof slab.

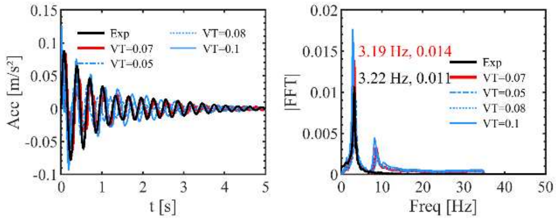

Figure 3. Comparison of numerical and experimental horizontal accelerations and FFTs from free vibration tests with a 1.18 kN load; VT varied (0.05–0.1), R_{inter} = 0.8.

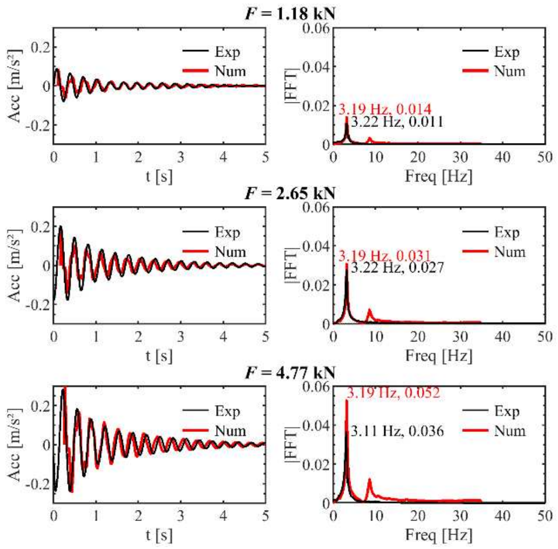

Figure 4. Comparison of numerical and experimental horizontal accelerations and FFTs from free vibration tests with loads of 1.18, 2.65, and 4.77 kN; R_{inter} = 0.8, VT = 0.07.

To compare numerical and experimental accelerations, the structural rotation angle ϑ was first calculated from the displacement components (horizontal u_x, vertical u_y) as $\vartheta = \tan^{-1}(u_y/u_x)$. This angle represents the instantaneous inclination of the structure. In the numerical model, horizontal acceleration a_x is computed along the global horizontal axis, assuming a purely horizontal force. However, experimentally the force generated by the rotating masses is inclined by ϑ because the masses rotate rigidly with the slab. Therefore, the actual force applied to the structure is not horizontal but acts at an angle ϑ, and the measured acceleration is along the rotated axis. To account for this, a simplified correction was applied by multiplying the numerical acceleration a_x by $\cos^2(\vartheta)$. The first $\cos(\vartheta)$ factor approximates the reduction of the effective horizontal force component due to the inclination of the applied load. This effectively reduces the numerical acceleration to represent the horizontal component of the actual inclined force without implementing an iterative load update. The second factor of $\cos(\vartheta)$ projects the acceleration vector onto the roof slab's inclined axis (to match the direction of experimental measurement). This approach enables a meaningful comparison between numerical results and experimental measurements.

Calibrating the interface parameters for the forced vibration tests was more challenging, as we aimed to achieve a good match between the accelerations at the top of the structure and the ground velocities measured 3 meters from the foundation edge. These quantities were recorded using an accelerometer placed at the top centre of the structure and a velocimeter in the surrounding soil. Using the same interface parameters calibrated from the free vibration tests (R_{inter} = 0.8, *VT* = 0.07) resulted in a less accurate simulation of the soil–structure interaction, leading to discrepancies in both the amplitude and frequency response (Figure 5). When applying a harmonic force at 3 Hz, the numerical accelerations at the top of the structure and the ground velocities were significantly higher than the experimental measurements. Conversely, for the 5 Hz input, the numerical acceleration at the top underestimated the experimental value, while the ground velocity—although still overestimated—was closer to the measured response than in the 3 Hz case. These differences suggest that the interface parameters derived from the free vibration case may not be suitable for accurately capturing the dynamic behaviour under forced loading conditions.

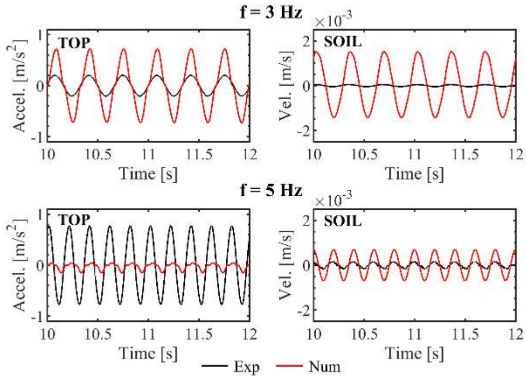

Figure 5. Numerical–experimental comparison of acceleration at the top of the structure and velocity in the soil (measured 3 m from the foundation edge) during forced vibration tests at 3 Hz and 5 Hz. Simulations were carried out using interface parameters calibrated from free vibration results (VT = 0.07; R_{inter} = 0.8).

Consequently, additional combinations of increased *VT* and decreased R_{inter} were tested to reduce the transfer of motion across the interface. Figure 6 presents the maxima of the accelerations projected on the roof plane and of the soil velocities obtained numerically for the 3 Hz case, compared with the experimental values (indicated by dashed lines). As an example, the numerical response at the foundation level is also shown, in comparison with the experimental results, to support the final assessment of interface performance. The combination *VT* = 0.385 and R_{inter} = 0.45 provided the best overall match, both at the top of the structure and in the soil and was therefore selected as acceptable for modelling dynamic soil–structure interaction. In this configuration, the numerical response at the foundation is slightly overestimated, suggesting that the PLAXIS interface model may not fully replicate the actual contact behaviour but is nonetheless effective in controlling wave propagation and energy transfer across the interface in the dynamic interaction problem.

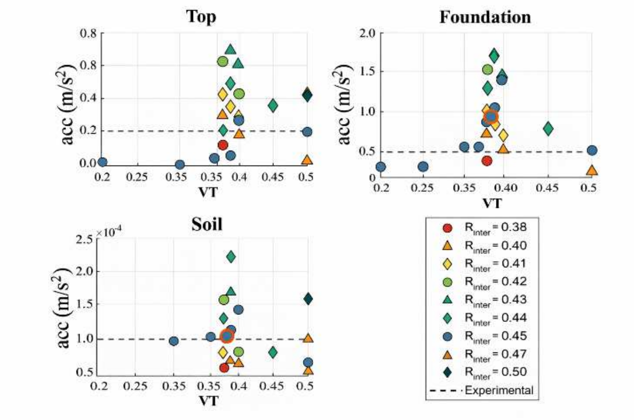

Figure 6. Comparison experimental vs numerical.

For the 5 Hz case, a similar parametric analysis was carried out, identifying $VT = 0.33$ and $R_{inter} = 0.6$ as the optimal combination for reproducing the experimental response at the top of the structure and in the soil. Finally, Figure 7 shows the related time histories at 3 Hz and 5 Hz with the optimal interface parameter to reproduce the experimental dynamic response. Table 3 summarizes the interface parameters representing the contact between concrete and soil in Layer 1 for the three cases analysed, which enable a good numerical-experimental fit. The observed variability reflects the dynamic impedance, which is frequency-dependent, as previously demonstrated by Amendola et al. (2021).

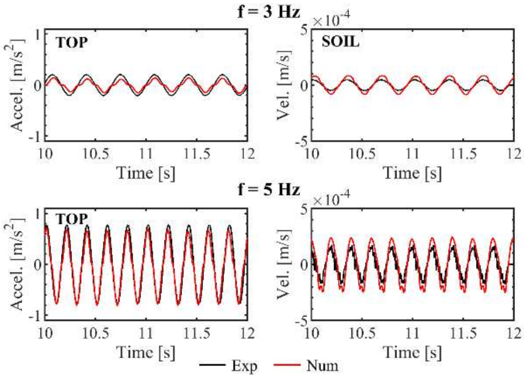

Figure 7. Numerical–experimental comparison of acceleration at the top of the structure and velocity in the soil (3 m from the foundation edge) during forced vibration tests at 3 Hz and 5 Hz. Results correspond to interface parameters VT and R_{inter} that provide the best fit from the parametric analysis (3Hz, VT = 0.385 and R_{inter} = 0.45; 5Hz, VT = 0.33 and R_{inter} = 0.6).

Table 3. Interface parameters

Dynamic analysis	*VT*	R_{inter}
Free Vibration	0.07	0.8
Forced Vibration 3 Hz	0.385	0.45
Forced Vibration 5 Hz	0.33	0.6

3 NUMERICAL PREDICTION OF THE EFFECT OF EPS LAYER AS GSI TECHNIQUE

With the numerical model calibrated in Section 2, a preliminary numerical investigation was carried out to evaluate the effectiveness of an expanded polystyrene (EPS) layer as a Geotechnical Seismic Isolation (GSI) technique. The simulated configuration included a 50 cm thick EPS slab placed beneath the foundation, extending 0.5 m beyond the foundation edges, for a total size of 4 × 4 × 0.5 m³. The main objectives were: (i) to verify that the EPS does not experience excessive deformation or failure under the static load of the structure, and (ii) to assess the dynamic response of the system with EPS—specifically, free vibration frequencies and recorded accelerations in the structure and soil—compared to the reference configuration without EPS, discussed in Section 2.

For constitutive modelling of EPS, we referred to an extensive experimental characterization campaign conducted by the Research Unit of Soil Dynamics and Earthquake Engineering at Aristotle University of Thessaloniki. This campaign included direct shear tests, oedometer tests, free expansion triaxial (TX) tests, bender element tests, and resonant column (RC) tests on EPS specimens with two nominal densities: EPS 150 (24 kg/m³) and EPS 200 (28 kg/m³) (Kroupi et al., 2024). In this study, simulations were performed using EPS 200. Based on the experimental results, we calibrated the parameters of the HS-small constitutive model. As no full-scale experimental data for EPS performance are yet available, a drained condition was assumed. Long-term strength parameters, derived from direct shear tests, were effective cohesion $c' = 56.4$ kPa and friction angle $\phi' = 3.4°$. To assess the influence of stiffness on the system response, two sets of deformability parameters were considered:

- Set 1: The stiffness moduli, including the small-strain shear modulus G0 and oedometric modulus Eoed, were computed using results from bender element and oedometer tests.
- Set 2: The stiffness parameters were derived from free expansion TX tests (E50).

In both sets, the reference shear strain γ0.7 was obtained from the shear modulus decay curves (G/G0) measured via RC tests. Using the experimentally derived values in each set, the remaining parameters required for the HS-small model were calculated based on the elastic modulus relationships described in Section 2.2. Table 4 presents the parameters directly obtained from tests (in bold) and the derived values for each set.

Table 4. Soil parameters. Bold values are from experimental tests; non-bold values were derived using the relationships in Section 2.2.

Set	v_s (m/s)	G_0 (kPa)	E_{ur} (kPa)	E_{50} (kPa)	E_{oed} (kPa)	$\gamma_{0.7}$ (%)
1	**410.6**	**4721**	2043	340.5	**672.2**	1
2	**-**	6000	16000	**8000**	16000	1

As for the interface between the EPS layer and the overlying foundation, contact now occurs between concrete and EPS, rather than between concrete and soil as in the reference configuration described in Section 2. Due to the lack of experimental data specific to this new interface, the same values of virtual thickness (*VT*) and interface reduction factor (R_{inter}) previously calibrated for the concrete–soil contact were adopted (see Table 3), acknowledging that they may not fully capture the real behaviour of the concrete–EPS interface.

Figure 8 shows the results of the stress–strain analysis under static loading conditions (i.e., application of the structure's self-weight), using the deformability parameters from Set 1, which yield the most demanding response. The vertical displacement at the top of the EPS slab remains below 8 mm (Figure 8a), while the vertical effective stress within the EPS reaches approximately 30 kPa (Figure 8b), well below the material's strength threshold (greater than 150 kPa). These results are encouraging with respect to the feasibility of safe experimental testing, as they indicate neither excessive settlement nor material failure under static loading.

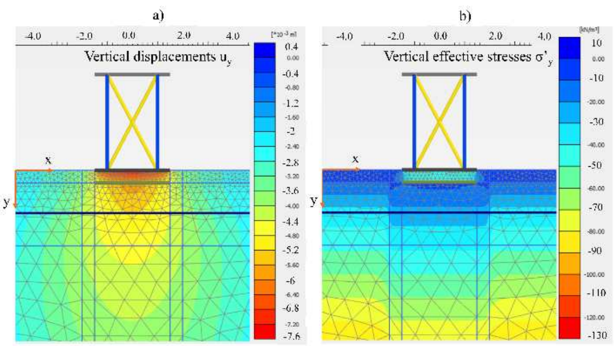

Figure 8. Results of the static loading analysis using EPS deformability parameters from Set 1: (a) vertical displacements u_y; (b) vertical effective stress distribution σ'_y.

Figure 9 presents a comparison of the dynamic response under free vibration (F = 4.77 kN) between the reference case without EPS (experimental data from the previous campaign) and numerical simulations with EPS using both deformability parameter sets. The acceleration time histories and corresponding FFTs clearly show a reduction in the fundamental frequency when EPS is present, due to its low density—approximately two orders of magnitude lower than the surrounding soil. Set 1, characterized by lower stiffness values, produces a more pronounced decrease in resonant frequency. In terms of amplitude, the acceleration is reduced with the inclusion of EPS.

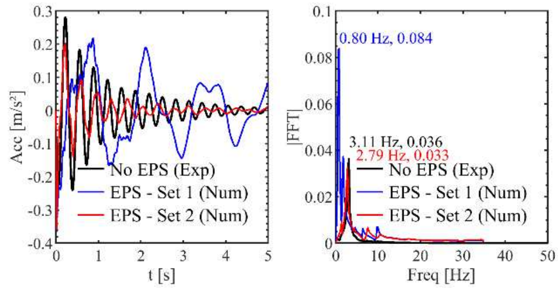

Figure 9. Comparison of acceleration time histories and FFTs under free vibration (with F = 4.77 kN) for the reference case without EPS and numerical simulations with EPS using both assumed deformability parameter sets.

Finally, Figure 10 compares the system's dynamic response under forced vibrations at 3 and 5 Hz for both parameter sets. Accelerations at the top of the structure and velocities in the soil are shown with and without the EPS layer. In all cases, the presence of EPS reduces the structural accelerations and ground velocities. If future experimental testing confirms that EPS behaviour aligns with Set 1 parameters, the highest reductions can be expected.

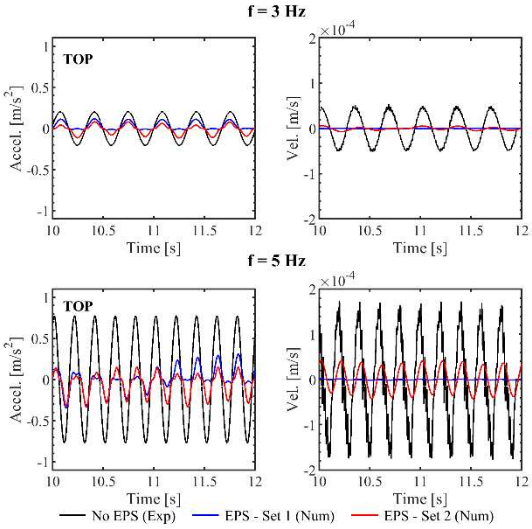

Figure 10. Accelerations at the top of the structure and soil velocities are shown with and without the EPS slab under forced vibrations at 3 Hz and 5 Hz. Results are presented for both deformability parameter sets of EPS assumed in this study.

4 CONCLUSIONS

The numerical results presented in this article show that EPS slab adopted as GSI technique can effectively modify the dynamic behaviour of the soil–structure system without undergoing excessive deformation or failure under static loading. These findings provide a solid basis for proceeding with the planned experimental campaign involving free and forced vibration tests on the EuroProteas structure equipped with an EPS layer. The upcoming experimental tests will be essential to select the most appropriate set of EPS deformability parameters by comparing numerical and experimental responses. Furthermore, they will allow for the calibration and validation of the interface parameters (VT and Rinter), which are currently assumed based on the reference configuration without EPS. Finally, the experiments will be instrumental in refining other numerical modelling aspects ensuring a reliable representation of the observed dynamic behaviour.

ACKNOWLEDGEMENTS

The authors gratefully acknowledge the Research Unit of Soil Dynamics and Earthquake Engineering at Aristotle University of Thessaloniki for conducting the experimental tests on EPS as part of the ERIES-POLIS project titled “POLystyrene for seismic ISolation: large-scale field testing of dynamic soil-foundation-structure Interaction of geotechnical seismic isolation (GSI) systems founded on expanded polystyrene (EPS).”

REFERENCES

Amendola, C., De Silva, F., Vratsikidis, A., Pitilakis, D., Anastasiadis, A. and Silvestri, F. (2021). Foundation impedance functions from full-scale soil-structure interaction tests. *Soil Dynamics and Earthquake Engineering*, 141: 106523.

Gatto, M.P.A., Montrasio, L. and Zavatto, L. (2021). Experimental analysis and theoretical modelling of polyurethane effects on 1D wave propagation through sand-polyurethane specimens. *Journal of Earthquake Engineering*. https://doi.org/10.1080/13632469.2021.1961933

Gatto, M.P.A., Lentini, V. and Montrasio, L. (2022). Dynamic properties of polyurethane from resonant column tests for numerical GSI study. *Bulletin of Earthquake Engineering*. https://doi.org/10.1007/s10518-022-01412-0

Gatto, M.P.A. and Montrasio, L. (2023). Artificial neural network model to predict the dynamic properties of sand-polyurethane composite materials for GSI applications. *Soil Dynamics and Earthquake Engineering*, 172: 108032.

Kroupi, G., Kapouniaris, A., Filoglou, E., Anastasiadis, A. and Pitilakis, D. (2024). Laboratory experiments of expanded polystyrene (EPS) – Scientific results of dynamic properties. *Internal Report*, Thessaloniki.

Lysmer, J. and Kuhlemeyer, R.L. (1969). Finite dynamic model for infinite media. *Journal of the Engineering Mechanics Division*, 95(4): 859–877.

Montrasio, L. and Gatto, M.P.A. (2016). Experimental analyses on cellular polymers for geotechnical applications. In: *Proceedings of the VI Italian Conference of Researchers in Geotechnical Engineering*, Bologna, Italy.

Pitilakis, K., Raptakis, D., Lontzetidis, K., Tika-Vasillikou, T. and Jongmans, D. (1999). Geotechnical and geophysical description of EUROSEISTEST, using field and laboratory tests and moderate strong motion records. *Journal of Earthquake Engineering*, 3(3): 381–409.

Pitilakis, D., Anastasiadis, A., Pitilakis, K. and Rovithis, E. (2013). Full-scale testing of a model structure in Euroseistest to study soil-foundation-structure interaction. In: *Proceedings of the 4th ECCOMAS Thematic Conference on Computational Methods in Structural Dynamics and Earthquake Engineering*, pp. 12–14.

Pitilakis, D., Rovithis, E., Anastasiadis, A., Vratsikidis, A. and Manakou, M. (2018). Field evidence of SSI from full-scale structure testing. *Soil Dynamics and Earthquake Engineering*, 112: 89–106.

Pitilakis, D., Anastasiadis, A., Vratsikidis, A., Kapouniaris, A., Massimino, M.R., Abate, G. and Corsico, S. (2021). Large-scale field testing of geotechnical seismic isolation of structures using gravel-rubber mixtures. *Earthquake Engineering & Structural Dynamics*, 50(10): 2712–2731.

Pitilakis, D., Anastasiadis, A., Vratsikidis, A. and Kapouniaris, A. (2024). Configuration of a gravel-rubber geotechnical seismic isolation system from laboratory and field tests. *Soil Dynamics and Earthquake Engineering*, 178: 108463.

Teshome, T.S. (2025). Comparative 2D finite element analysis of soil–cement block and column reinforcements for deep excavation support. *Engineering Reports*, 7: e70275.

Tsang, H. (2025). Geotechnical seismic isolation (GSI): State of the art. *Soil Dynamics and Earthquake Engineering*, 198: 109627. https://doi.org/10.1016/j.soildyn.2025.109627

Obrzud, R.F. and Truty, A. (2018). The Hardening Soil Model – A Practical Guidebook. ZSoil, Lausanne. Available at: https://www.zsoil.com/zsoil_manual_2018/Rep-HS-model.pdf (Accessed 29 July 2025).